THE EFFECT OF PARTICLE SHAPE ON SOLUTE DISPERSION IN LIQUID-SOLID CHROMATOGRAPHIC COLUMNS

Thesis for the Degree of M. S.

MICHIGAN STATE UNIVERSITY

Joseph F. Gentile

1966

ABSTRACT

THE EFFECT OF PARTICLE SHAPE ON SOLUTE DISPERSION IN LIQUID-SOLID CHROMATOGRAPHIC COLUMNS

by Joseph F. Gentile

As part of a continuing effort to develop a reliable scale-up procedure for liquid-solid chromatographic separations the effect of particle shape on axial dispersion in packed beds has been investigated.

The pulse input method was used in calculating the axial dispersion coefficients. These calculations were accomplished by obtaining solute (NaCl) concentration versus time data at two positions in a bed of irregularly shaped glass particles. Concentrations were measured by electrolytic conductance at the two measuring points.

In order to correlate the data from this work with those obtained in a similar investigation involving beds of spheres, it was necessary to determine experimentally an effective diameter for the nonspherical particles. The effective diameter was defined as the diameter a sphere would need in order to possess the same surface area as the irregular particle.

Using this basis for diameter comparison, it was found that for flow rates between one and one-hundred feet per hour the axial dispersion coefficient for a bed of randomly shaped particles was significantly higher than that for a similar bed of spheres.

THE EFFECT OF PARTICLE SHAPE ON SOLUTE DISPERSION IN LIQUID-SOLID CHROMATOGRAPHIC COLUMNS

By

Joseph F. Gentile

A THESIS

Submitted to
Michigan State University
in partial fulfillment of the requirements
for the degree of

MASTER OF SCIENCE

Department of Chemical Engineering

1966

To My Mother and Father

ACKNOWLEDGMENT

The author gratefully acknowledges the Upjohn Company and the National Science Foundation for the financial support of this work.

Sincere appreciation is also extended to Dr. Martin C. Hawley for his invaluable assistance and guidance during the course of the project.

TABLE OF CONTENTS

TABLE OF CONTENTS

LIST OF TABLES

LIST OF TABLES

LIST OF FIGURES

FIGURES

FIGURE | PAGE

INTRODUCTION

Dispersion in fluid flow through porous media has been the subject of intensive study by scientists and engineers for many years. Several transport theories, such as the mixing cell model,[9] the diffusion model,[11] and the statistical approach,[8] have resulted from this effort and have become invaluable in predicting the outcome of various experiments. These findings, for example, have aided in the development of such processes as extraction, drying, and absorption.

However, the pharmaceutical industry, which uses the separation technique known as chromatography for large-scale production, has been unable to scale-up chromatrographic separations reliably. That is, the current theories did not satisfactorily account for the several processes (fluid flow, absorption, and desorption) which occur simultaneously within the bed. It was therefore necessary to review the various hypotheses in so far as they pertained to chromatography.

Previously, theoreticians treating the phenomena of mass transfer and fluid flow through porous media have worked only with packed beds comprised of tiny spherical particles. In chromatography, however, the shape of the packing material usually employed is highly irregular (microphotographs of two of these materials, activated carbon and diatomaceous earth, appear in the Appendix as Figure I-I and I-II, respectively). For this reason a study of the effect of particle shape on fluid flowing through a packed bed was initiated.

[illegible]

[illegible] in fluid flow [illegible]
of intensive study by scientists [illegible]
transport theories, such as [illegible]
and the statistical approach,[9] [illegible]
become [illegible] in predicting the [illegible]
fluidizers, for example, [illegible]
extraction, drying, and [illegible].

However, the phase [illegible]
technique known as chromatography [illegible]
to molecular-thermodynamic expressions [illegible]
theories did not satisfactorily account for [illegible]
time, [illegible]
It was therefore necessary to [illegible]
they pertained to chromatography.

Previously, [illegible]
and fluid flow through porous [illegible]
properties of the [illegible]
Since of the [illegible]
([illegible] of [illegible]
earth, appear in the [illegible], respectively. For
this reason a study of the [illegible] fluid flowing
through a packed bed [illegible].

An investigation of this nature is necessarily empirical. That is, the mathematics describing axial dispersion in fluid flow through a column filled with an irregularly shaped packing material is sufficiently complicated that the problem has not been solved. However, a qualitative theoretical discussion will be presented.

THEORETICAL DISCUSSION OF THE PROBLEM

It is first necessary to present the mathematical treatment of axial dispersion in plug flow through a packed bed.

The second section of this discussion will deal with the mixing cell model of dispersion in packed beds.[1,10] Although other theories have proved equally capable in explaining this phenomenon, the mixing cell model is especially convenient for the qualitative presentation given below. A latter portion of this section will consider the theoretical effect of particle shape on the axial dispersion in packed beds.

Dispersion in a Non-adsorbing Bed

Consider a packed bed comprised of a non-adsorbing material, with concentration measuring devices located at X_o and X_1 (Figure I).

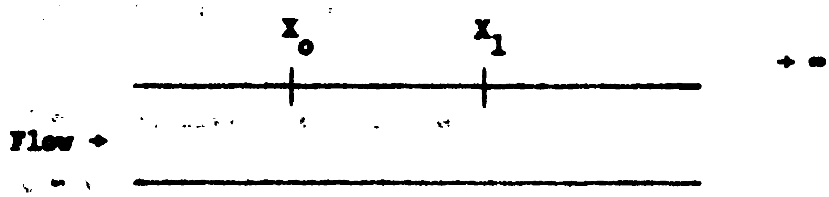

Figure I. Diagram of Bed

Solvent is continuously flowing through the bed with a volumetric flow rate W. A pulse of tracer solution is injected into the column upstream from X_o and allowed to pass through the bed. Associated with the packed section is an axial dispersion coefficient, D.

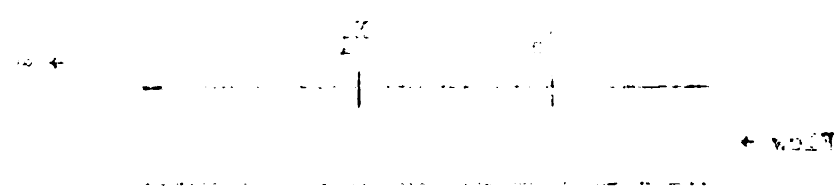

It is necessary to assume:

1. The tracer is injected uniformly across the bed.

2. The flow is uniform over the cross section of the bed.

3. The amount of mass transfer by dispersion is proportional to the axial concentration gradient, $\frac{\partial C}{\partial X}$.

C is the average concentration of tracer across a section of the column.

The equation describing this phenomenon is obtained from a material balance of tracer on an incremental length of packed bed (Figure II):

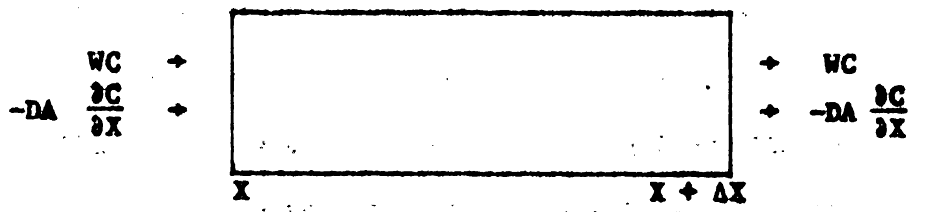

Figure II. Increment of Bed

$$\frac{\partial^2 C}{\partial X^2} - \frac{W}{D\varepsilon A}\ \frac{C}{X} = \frac{1}{D}\ \frac{\partial C}{\partial t} \qquad (1)$$

where X = axial distance variable

t = time

ε = void fraction of bed

A = cross sectional area of column

The boundary conditions are:

$c = o$ when $t = o$ for $x \geq X_o$

at $X = X_o$ $C = C_o(t)$ for $t > o$

at $X = \infty$ $C(t)$ = finite for $t \geq o$

Hawley[6] has shown that

$$\psi = \frac{2\varepsilon AD}{WL} \qquad (2)$$

$$L = X_1 - X_o \tag{3}$$

where ψ is a measure of the spread of the pulse due to axial dispersion and is defined as

$$\psi = \frac{(\sigma_1^2 - \sigma_o^2)}{(\mu_1 - \mu_o)^2} \tag{4}$$

σ_i^2 is the time variance of the concentration at X_i and μ_i is the mean time concentration at X_i.

This, in effect, states that the spread due to dispersion is proportional to the axial dispersion coefficient.

This model is based on assuming plug flow with axial dispersion. Even if the flow does not approximate plug flow, it is assumed that these irregularities are accounted for by the axial dispersion coefficient.

The Mixing Cell Model and the Effect of Particle Shape on Dispersion

Any packed bed, of necessity, is comprised of a series of randomly oriented void spaces. These voids, usually referred to as mixing cells, are arbitrarily shaped and sized. However, it will be convenient to consider a column consisting of mixing cells of approximately equal volume.

The fluid passing through the bed is usually considered as many differential elements of liquid passing from one void to another. The period of time a fluid element is present in the i^{th} mixing cell is defined as the residence time for that particular void and is denoted by θ_i.

For the case of piston flow through the bed with perfect mixing in each cell

$$\theta_1 = \theta_2 = \ldots = \theta_i = \ldots = \theta_n = \text{constant} \tag{5}$$

That is, the residence time for each void is a constant. This situation requires the absence of back and forward mixing, so in effect for $n \to \infty$, the dispersion is zero.[4]

If each mixing cell is assumed to be a site of perfect mixing, the dispersion will increase as $n \to 1$. That is, for the case of an unpacked, perfectly mixed channel the dispersion would be infinite. Carberry[3] has reported quantitative evidence of this relationship between the dispersion and n. It is important to reiterate that these conclusions are valid only for beds containing perfect mixing cells with constant residence times.

If perfect mixing does not occur within the voids of a bed

$$\theta_i \neq \theta_k \text{ when } i \neq k, \tag{6}$$

in general, and a residence time distribution results. As this distribution becomes more pronounced the amount of intercellular mixing, and consequently, the dispersion, increases. This situation is usually created when intracellular mixing efficiencies are low.[4]

The term mixing efficiency is employed as an indication of the degree of mixing occurring within a void space. The mixing efficiency, E, is a maximum when perfect mixing is present. Clearly, then, the cell mixing efficiency is an inverse function of the cell size and is directly related to fluid turbulence. Some measure of the relative cell sizes for two or more packed beds can be obtained by measuring the void fraction of the packings. The dispersion will then, in effect, be directly related to the void fraction.

Turbulence will be some complex function of the fluid velocities and velocity gradients within the bed. Unlike the velocity gradients the fluid velocities can usually be closely approximated by the average

interstitial velocity through the column. Velocity gradients can only be obtained if the flow profile through the bed is known.

Such a profile is not available since such a mathematical analysis would require a precise description of an arbitrarily shaped particle. However, it is possible to discuss the characteristics of flow about a single irregular particle relative to that of a sphere.

The streamlines for flow around a sphere are shown in Figure III.[5] Significant velocity gradients can only be found on streamlines near the surface of the sphere.

Figure IV is a similar drawing of streamlines about a non-spherical particle. The overall effect of the irregular particle on the fluid is essentially the same as that of the sphere. However, near the surface of the particle there is a substantial increase in the amount of stagnant fluid present. This is primarily caused by surface cracks, ragged edges, and projections from the particle. It is also possible that the turbulence downstream from the irregular particles would be somewhat greater than the turbulence created by the sphere.

If the effect of the increased amount of stagnant fluid predominates, in a packed bed there will be less turbulence in the voids made by irregular particles than in the void cells created by spheres. Consequently, there is less mixing within each irregular cell. As discussed previously, this results in a broadening of the residence time distribution for the n mixing cells within the bed. The overall effect is an increase in the amount of intercellular mixing and is observed experimentally as an increase in the dispersion coefficient. This is true since mixing, and thus dispersion, in the mixing cell model is related to the dispersion coefficient in the dispersion model.

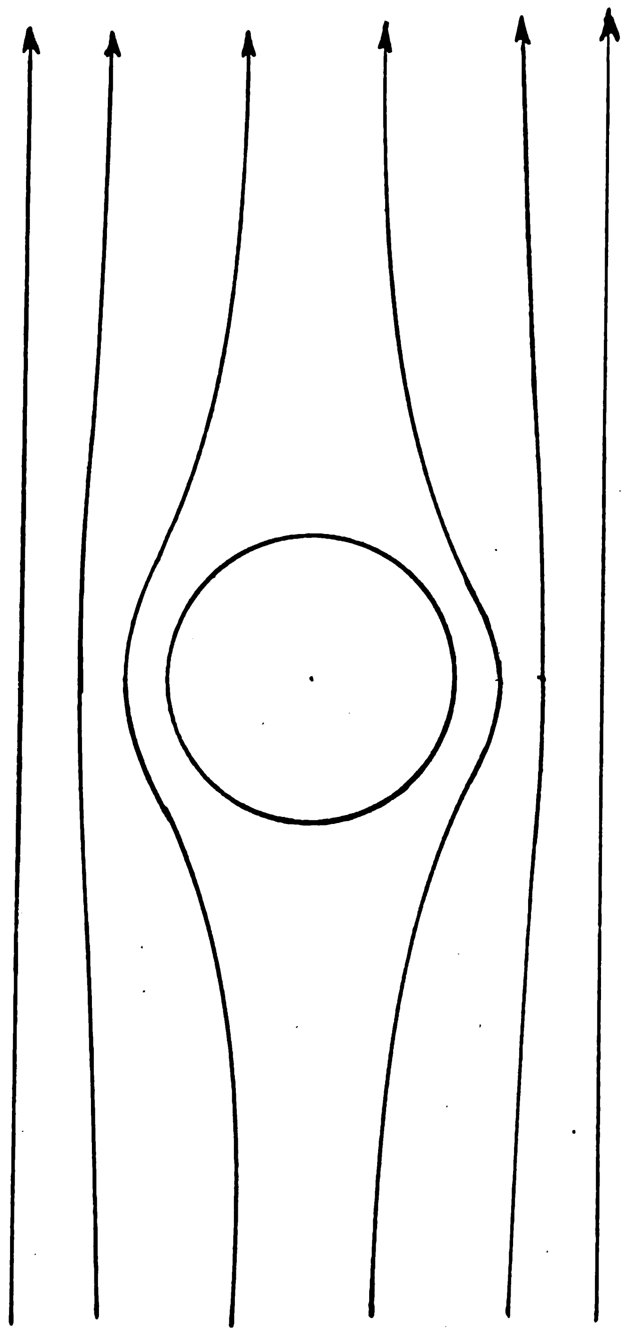

Figure III. Flow Around A Sphere

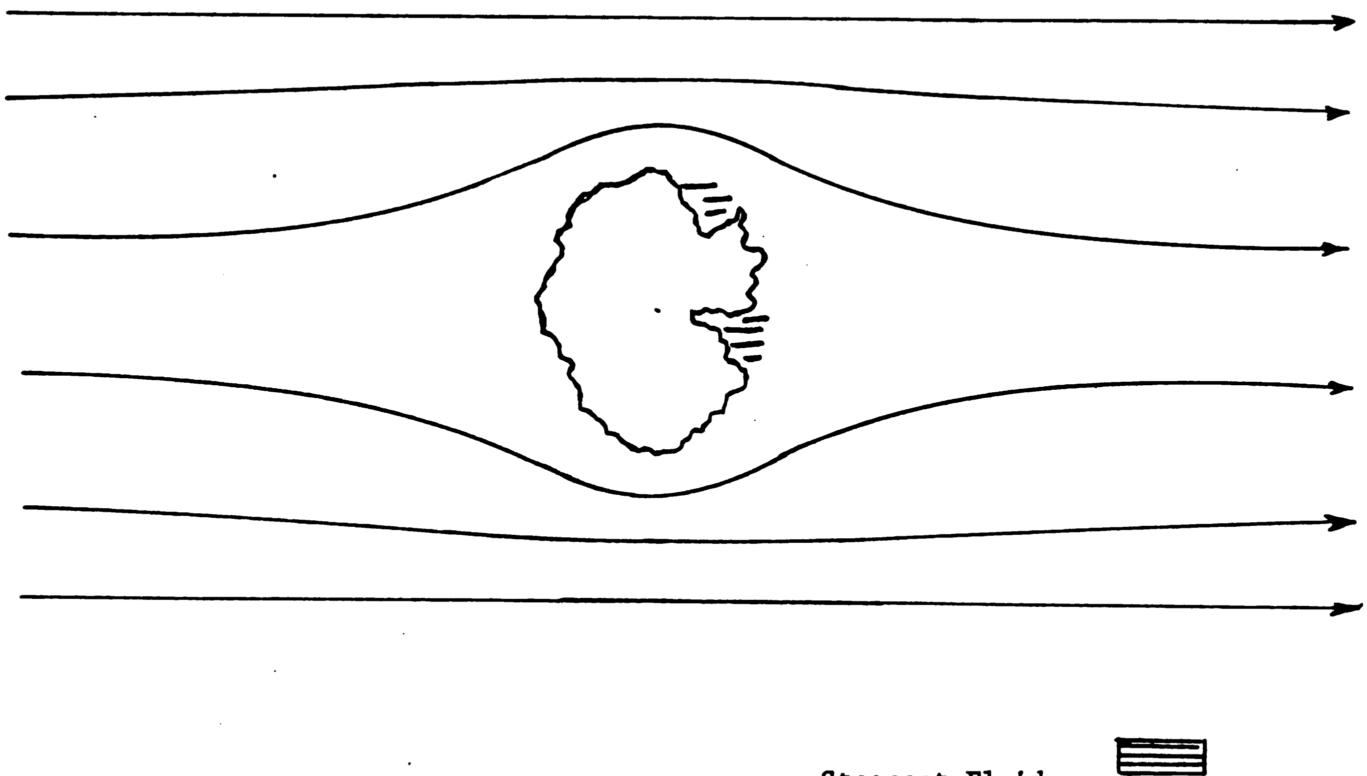

Figure IV. Flow About an Irregular Particle

Conversely, if the increased turbulence is more significant than the extra stagnant fluid, the dispersion coefficient for a bed of irregular particles will be less than that for a bed of spheres. That is, the added agitation within a mixing cell produces a greater intracellular mixing efficiency causing less intercellular or bulk mixing, and consequently a smaller dispersion coefficient.

EXPERIMENTAL METHOD

The apparatus used for this experimentation consisted of a one-half inch diameter glass column, a pressurized flow system, and two conductivity cells which, together with an automatic recorder, measured tracer concentration versus time.

The Flow System (Figure V)

The column was an 18-inch length of flanged pyrex pipe. One-quarter inch tubing was used to connect the water and tracer supply tanks to the column. A galvanized steel tank was used to store the water while the tracer solution was kept in a stainless steel vessel. Nitrogen was used to maintain pressure throughout the system. Flow rates were adjusted using a micrometer valve located on the downstream side of the column.

Conductivity Cells (Figure VI)

Conductivity cells identical to those designed by Hawley[6] were employed. The cell was machined from plexiglass to the specifications indicated in Figure VI. The wire was No. 25 platinum wire.

It was also necessary to place a small circular section of filter cloth over the cell to prevent the packing material from entering the measuring device.

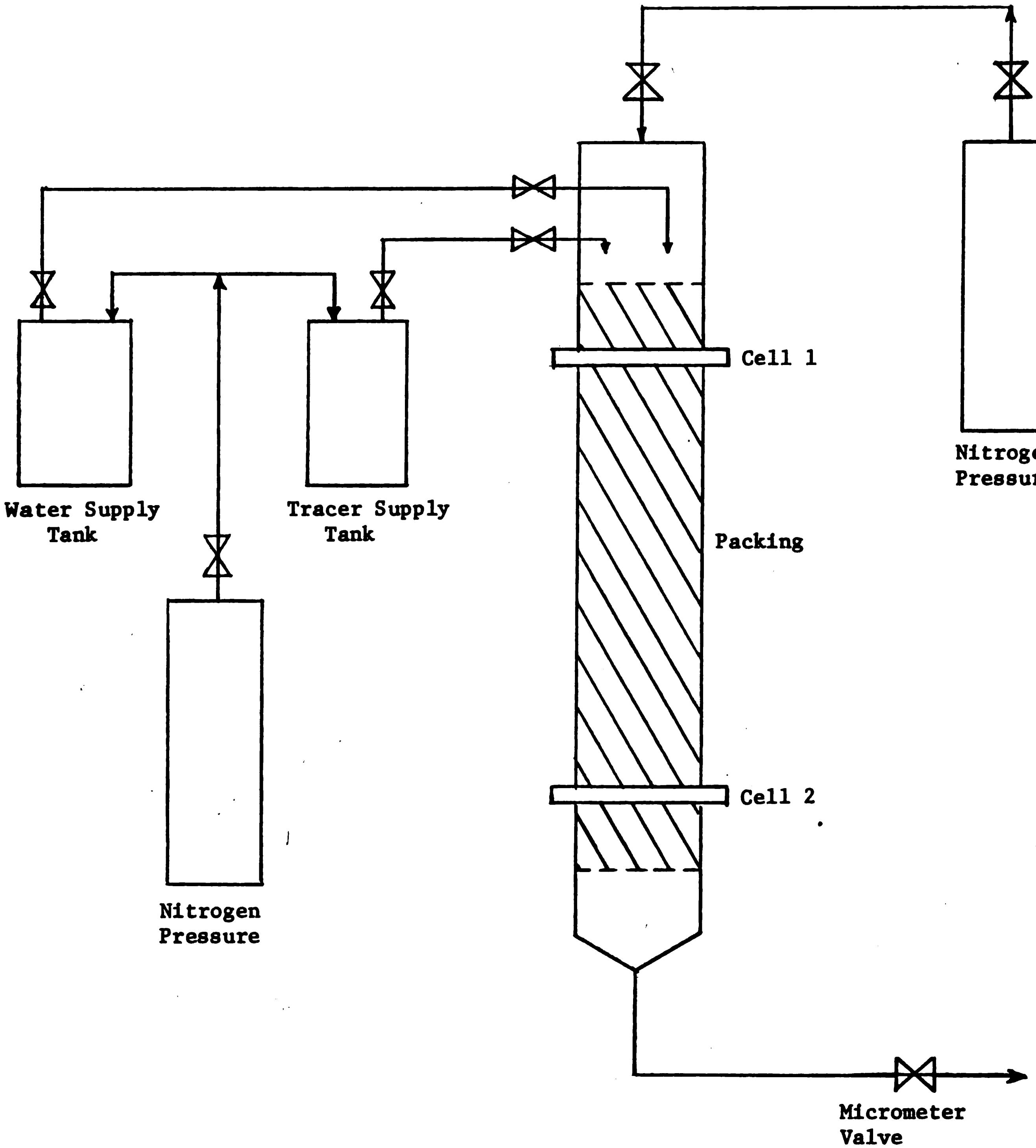

Figure V. Schematic of Flow System

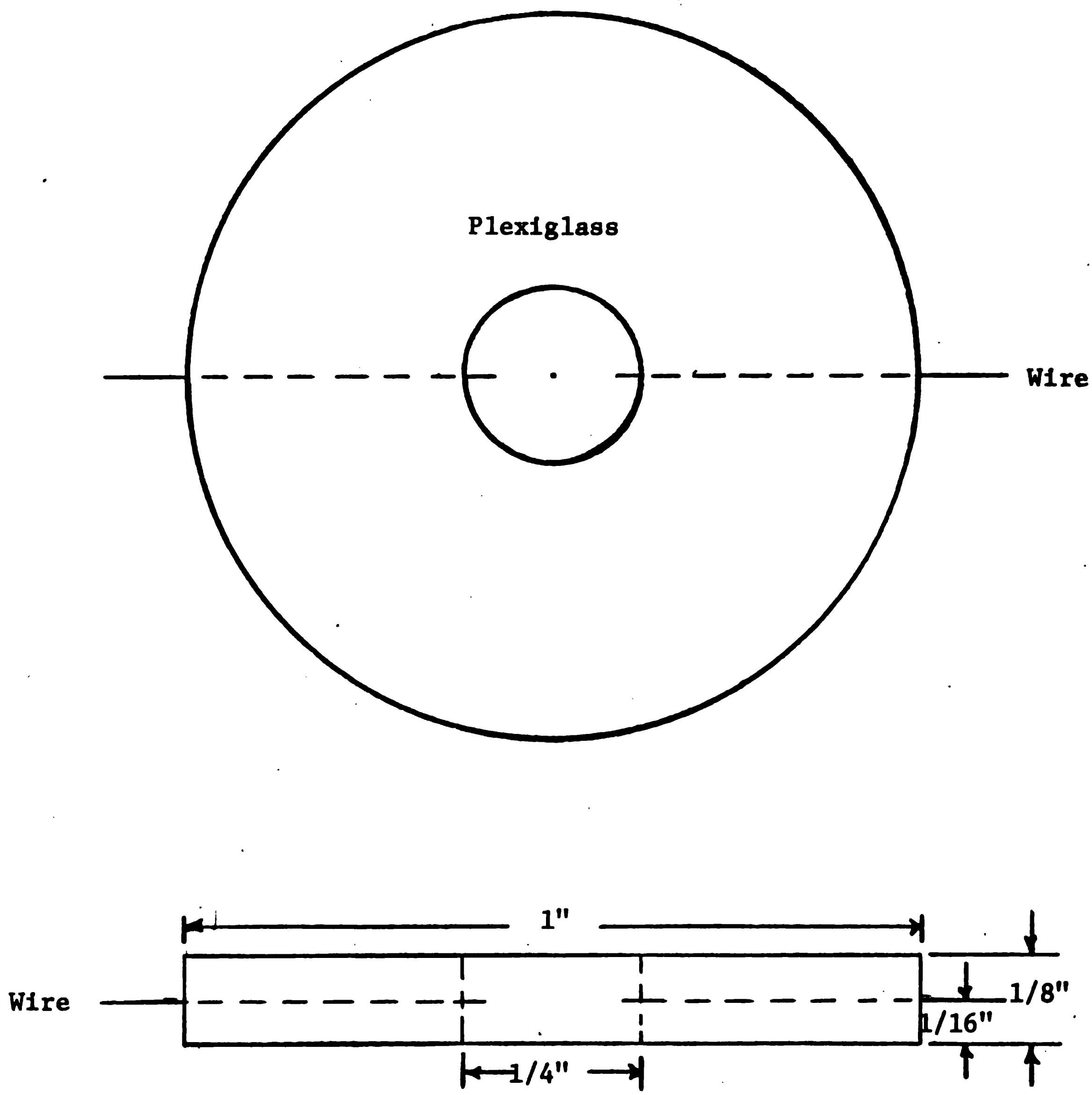

Figure VI. Conductivity Cell

Tracer Solution

An aqueous sodium chloride solution was chosen as a tracer since NaCl concentrations can be readily determined by electrolytic conductance. Also, the specific conductance of sodium chloride is proportional to its concentration in the range of 0 to 700 parts per million.[6] Tracer concentrations for this work were approximately 0.5 g./l. or about 500 parts per million.

For a concentration of 0.5 mol/l. at 30°C the molecular diffusivity D_v is 1.84×10^{-5} cm^2/sec.[7]

Measuring and Recording Apparatus (Figures VII & VIII)

In order to measure and record the tracer concentration as a function of time the circuitry designed by Hawley,[6] and shown in Figure VII was used.

The voltage drop across resistor R is proportional to the reciprocal of the cell resistance R_c, and is given by

$$E = I\ R \qquad (7)$$

where

$$I = v/(R_c + R) \qquad (8)$$

However, R is designed to be much less than R_c so that

$$E = V\ R\ /\ R_c \qquad (9)$$

Both V and R are constant so E is then proportional to $1/R_c$ for $R_c \gg R$.

The voltage was supplied by a variable frequency audio oscillator. The A.C. voltage across R was then amplified, rectified, and measured with a

Sargent multi-range recorder, as shown schematically in Figure VIII.

The Packing Material

Difficulty was encountered in obtaining irregularly shaped glass particles with diameters between 0.0098 and 0.0070 in. (60 and 80 mesh). Glass raschig rings were crushed in ball mills (using wet and dry procedures), and in rotary grinders, but in both cases the particles were too large, and nearly spherical. Prolonged processing pulverized the material.

Satisfactory results were obtained, however, with a mortar and pestle. Microscopic examination showed the shape of the packing material to be highly irregular. Microphotographs of the spherical and non-spherical particles appear in the Appendix as Figures I-III and I-IV, respectively.

After crushing, the material was screened in order to obtain those particles with maximum diameters between 60 and 80 mesh.

The average void fraction of the packed bed was found to be 0.45 by the displacement of water.

Determination of Effective Particle Diameter

The size of the irregular particles was originally determined by measuring the maximum particle diameter, or more precisely, the maximum cross-sectional distance. Unlike the spherical case, the maximum diameter (d_{max}) for the irregular bead did not necessarily present a true picture of the particle (Figure IX). Therefore, to compare effectively the diffusivity data for the spherical and non-spherical packings, a diameter other than d_{max} was required.

Roemer[12] reported that the diffusivity was a function of the particle diameter and was therefore related to the surface area of the packing

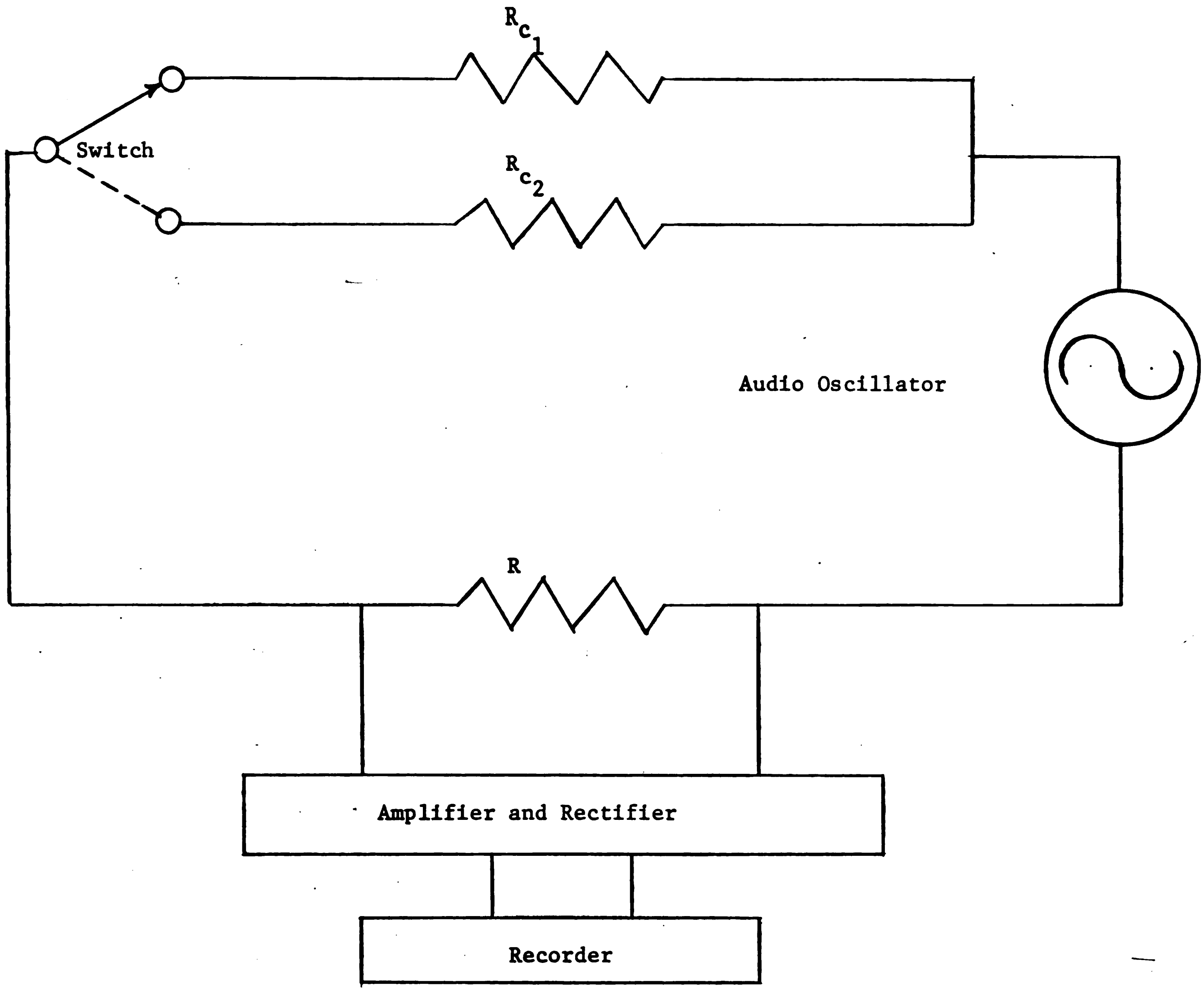

Figure VII. Schematic of Electrical Circuit for Conductivity Measurements

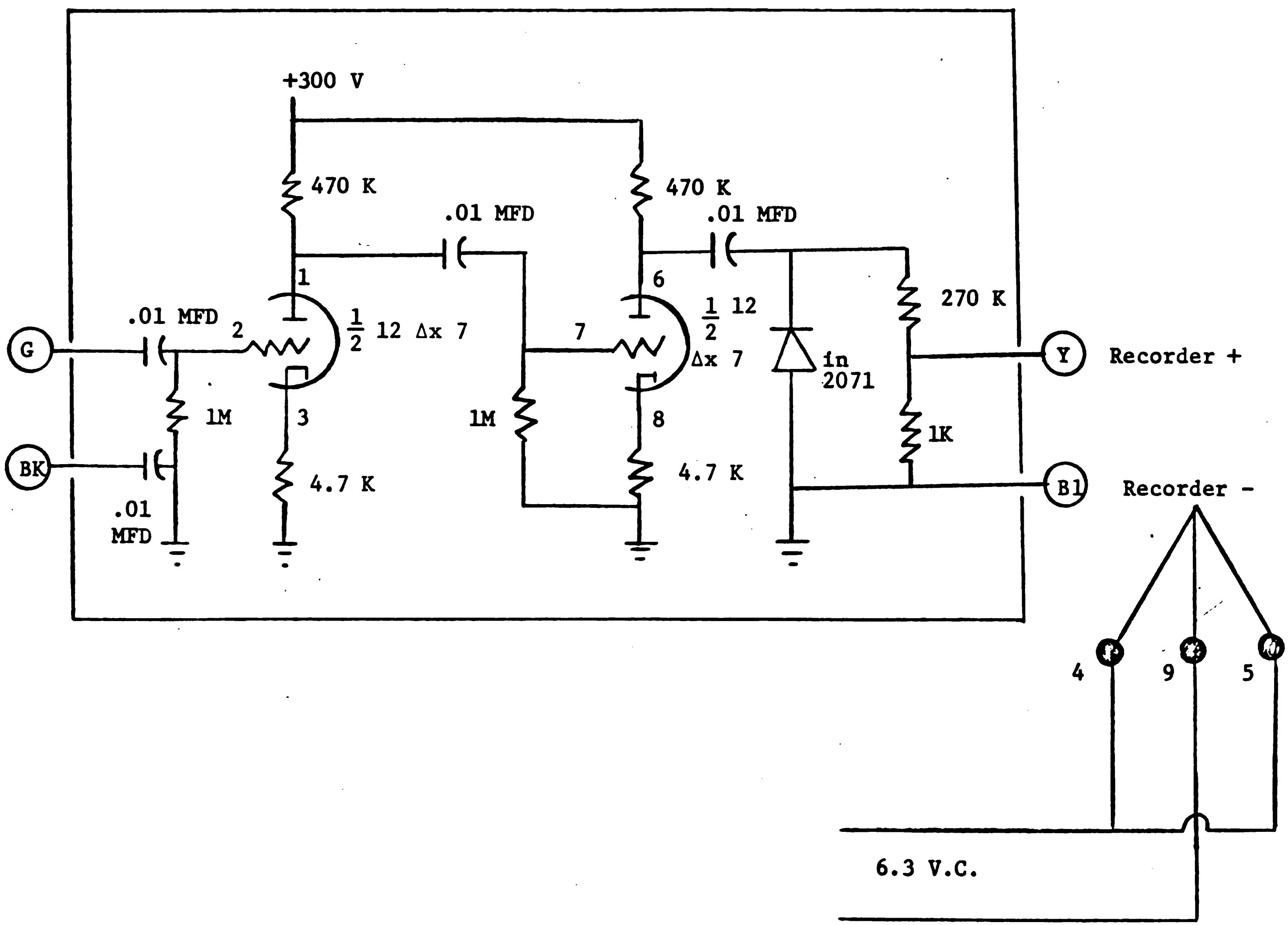

Figure VIII. Schematic of Rectifying Amplfying Circuit

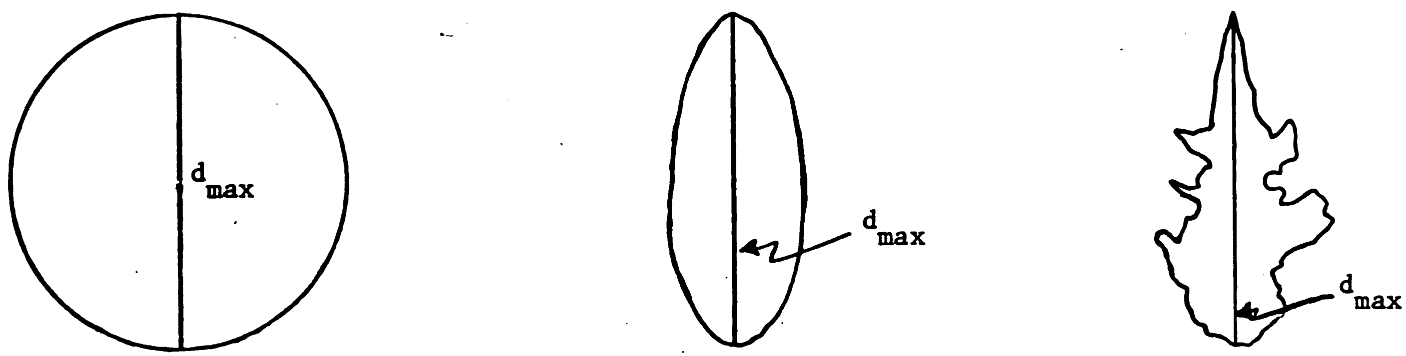

Figure IX. Three Dissimilar Particles with Equal Maximum Diameters exposed to the flowing medium. Consequently, it was decided to calculate an effective particle diameter which was defined as the diameter a sphere would need to possess the same surface area as the irregular particle. A bed of spheres with diameters equal to the effective diameter (d_{effec}) would then have a total surface area identical to that of the bed of irregular particles.

Determination of the effective diameter was facilitated by the Blake-Kozeny relationship:[2]

$$d^2 = \frac{150\ V_o\ L\ \mu(1 - \epsilon)^2}{\Delta P\ \epsilon^3\ g_c} \tag{10}$$

where d = diameter, feet

V_o = flow rate of liquid through bed, ft/hr.

L = length of bed, feet

μ = viscosity of flowing medium, lb/ft.hr.

ϵ = void fraction of bed

ΔP = pressure drop across bed, lb/ft.^{2}

g_c = gravitational constant, lb force ft/lb. mass sec.^{2}

This equation relates particle surface area to the pressure drop across the packed bed. Since Equation (10) assumes the packing particles are spherical, the effective particle diameter is obtained directly. That is

$$d^2 = (d_{effec})^2 \tag{11}$$

A schematic diagram of the apparatus necessary for this determination is depicted in Figure X. As before water was used as the flowing medium and nitrogen was employed to pressurize the system.

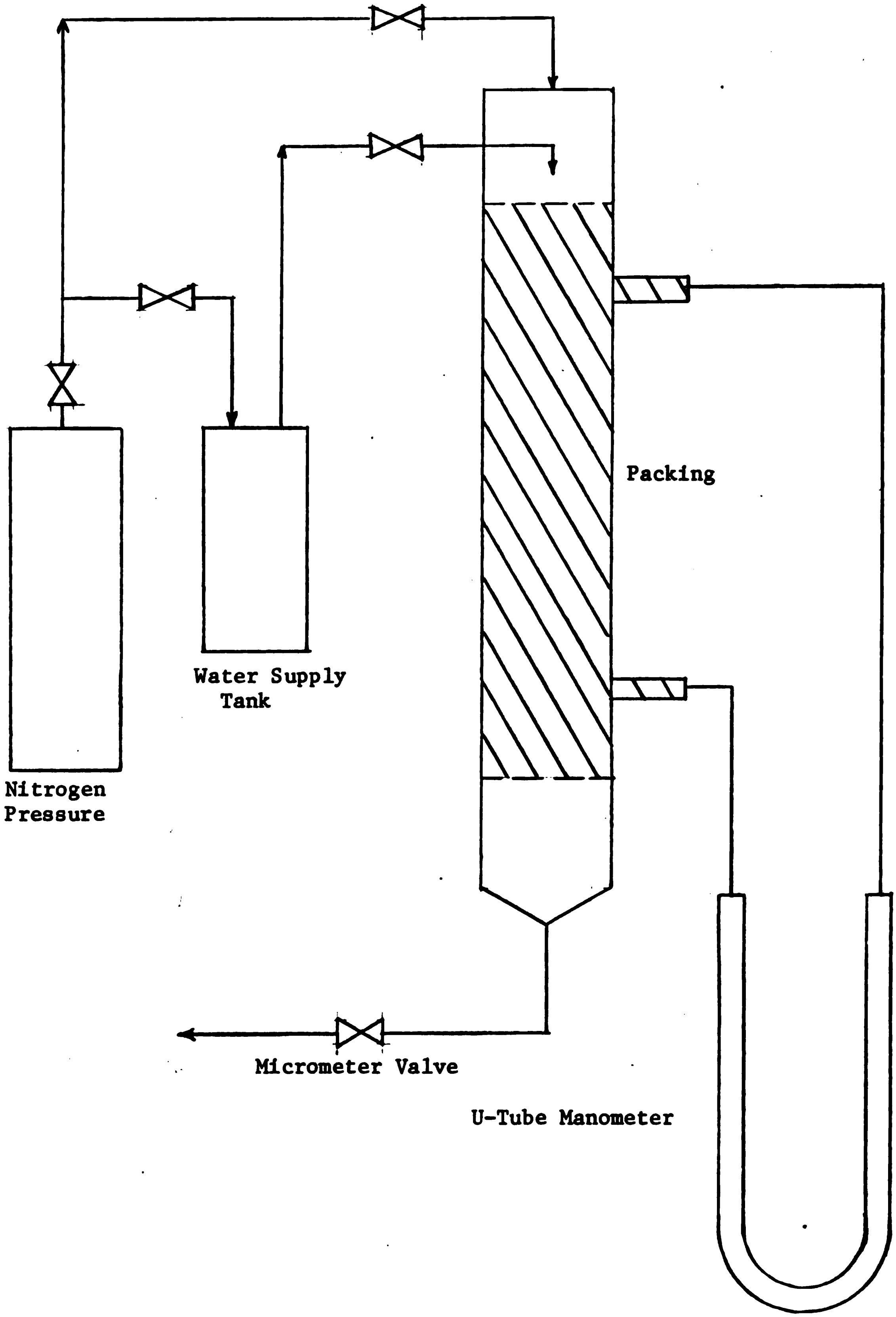

Figure X. Schematic of Equipment to Measure Pressure Drop

Packing Procedure

For effective operation it was essential that the column be free of trapped air and unpacked channels. Air entrappment was eliminated by slurrying the packing material in water and channeling was prevented by vibrating the column as it was filled. In addition, each portion of the column was filled with water before packing was initiated.

After the bottom section was satisfactorily packed a conductivity cell, together with its filter cloth cover, was fastened between the top of this portion and the bottom of the next. Having repeated the above procedure for the second segment of the column, the third and uppermost section was packed to a height of two inches above the top conductivity cell.

Finally, a circular piece of 60 mesh screen, which served as a liquid distributor, was placed on top of the bed.

Run Procedure

Distilled water was permitted to flow through the bed until constant zero readings were obtained from each conductivity cell. The water level was then allowed to drop to the top of the bed, at which point the flow was stopped by closing the micrometer valve. A pulse of tracer solution, which was carefully introduced into the column, was allowed to enter the bed by regulating the liquid flow rate. The water supply and micrometer valves were then opened to obtain the desired rate of flow through the bed.

As the tracer passed through the column conductance versus time measurements were recorded from both cells. To insure that conductance was proportional to the scale readings resistance versus recorder readings were obtained prior to and after each run.

Packing Procedure

For effective operation it was [illegible]
trapped air and uncoated crystals. [illegible]
slumping the packing material is [illegible]
vibrating the column as it was filled [illegible]
column was filled with water before [illegible]

After the bottom section was [illegible]
cell, together with its filter cloth [illegible]
of this portion and the bottom of the [illegible]
procedure for the second segment of the [illegible]
section was packed to a height of two [illegible]

Finally, a circular piece of [illegible]
liquid distributor, was placed on top of [illegible]

[illegible]

Distilled water was permitted to [illegible]
zero readings were obtained from each [illegible]
was then allowed to drop to the top of [illegible]
stopped by closing the outlet water valve. A [illegible]
was carefully introduced into the column, [illegible]
regulating the liquid flow rate. The water [illegible]
were then opened to obtain the desired rate of flow [illegible].

As the tracer passed [illegible]
[illegible] cells. [illegible]
was proportional to the [illegible]
were [illegible]

Calculation of the Dispersion Coefficient

Hawley[6] showed that the dispersion coefficient D could be calculated from the relation

$$\frac{\sigma_2^2 - \sigma_1^2}{(\mu_2 - \mu_1)^2} = \frac{2D}{UL} \qquad (12)$$

where u is the interstitial velocity

$$\mu_n = \int_0^\infty Ct\ dt \Big/ \int_0^\infty C dt \qquad (13)$$

and

$$\sigma_n^2 = \int_0^\infty C(t - \mu_n)^2\ dt \Big/ \int_0^\infty C dt \quad n = 1,2 \qquad (14)$$

The subscripts 1 and 2 refer to the upper and lower conductivity cells respectively.

Numerical solutions to the above integrals were obtained through the use of Simpson's Rule and a Control Data Corporation 3600 Digital Computer.

The computer input consisted of scale readings obtained from the recorder chart at equally spaced time increments. The values used were simply the actual scale readings minus the zero point.

Since corrected scale readings were proportional to tracer concentration they could be used in place of C in Equations 13 and 14.

Also, Hawley[6] reported that since σ_n^2 was independent of the reference time utilized the time could be considered as zero at the beginning of each cell. The time between the beginning of the two measuring points was noted, however, and added to μ_2 for the final calculation of D.

The interstitial velocity was calculated using

$$U = L/ (\mu_1 - \mu_2) \tag{15}$$

The conductance versus time measurements for a typical experimental run are plotted in Figure XI.

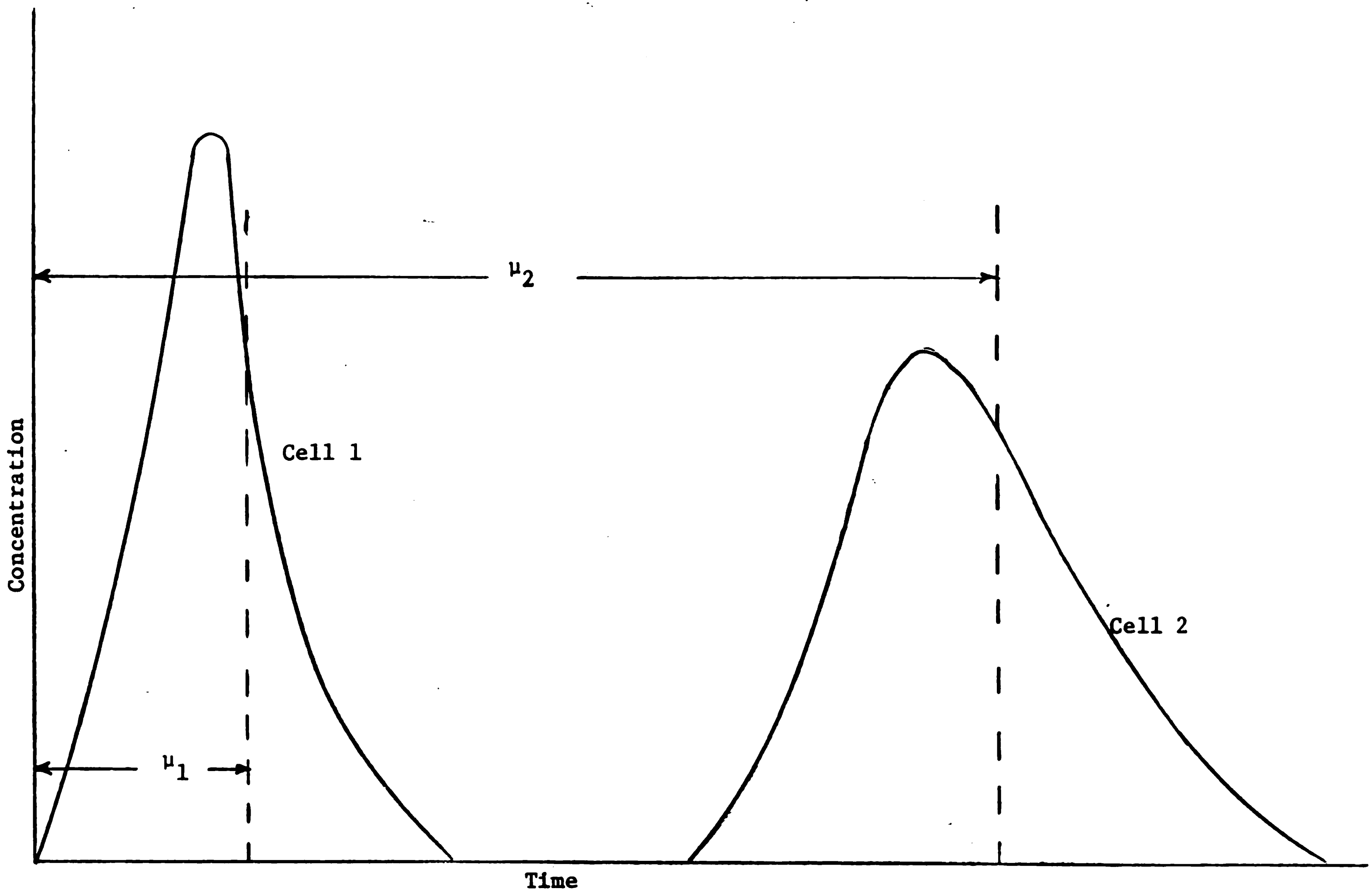

Figure XI. Typical Concentration vs Time Curves for Cells 1 and 2

PRESENTATION OF DATA

Correlation Methods

It has been reported that for fluid flow in a packed bed a log-log plot of D/D_v versus $d_t\ u/D_v$ should be a straight line. This is due to the similarities in the relationships for the eddy diffusivity for turbulent flow,[13] and the axial diffusivity for laminar flow,[14] in a tube (Equations 16 and 17).

$$D = 3.7\ d_t\ u\ \sqrt{\gamma} \tag{16}$$

$$D = d_t^2\ u^2/192\ D_v \tag{17}$$

where γ = resistance coefficient

d_t = tube diameter

To facilitate proper data correlation for the packed column it was necessary to substitute four times the hydraulic radius for the tube diameter. Thus, for a bed packed with spheres

$$d_t = 4M = \frac{2}{3}\ \frac{\epsilon}{1 - \epsilon}\ d_{effec} \tag{18}$$

It is correct to use the hydraulic radius for spheres since d_{effec} is calculated with the assumption that the packing particles are spherical.

A plot of log D/D_v versus log $4Mu/D_v$ is depicted in Figure 12 for the data obtained from this investigation. For comparison the data reported by Hawley[6] are also presented on this graph.

In addition, a plot of log D versus log u for the same sets of data, is presented in Figure XIII.

[illegible]

[illegible]

It has been reported that [illegible] plot of [illegible] versus $L_f\,u/D_v$ [illegible] similarity, in the mixing [illegible] flow,[15] and the axial diffusivity for [illegible] 16 and 17).

$$D = 3.7\, d_e\, u \sqrt{\gamma} \qquad [illegible]$$

$$[illegible] = d_e^2\, u^2 / 1.2\, [illegible] \qquad [illegible]$$

where γ = [illegible] coefficient

d_e = [illegible] diameter

To [illegible] proper data [illegible] it is necessary to substitute for [illegible] the hydraulic [illegible] diameter. Thus, for a bed [illegible]

$$d_e = [illegible] \qquad [illegible]$$

It is correct to use [illegible] is calculated with [illegible] equation.

A plot of log D/D_v versus [illegible] Figure [illegible] for the data obtained from [illegible] by Bailey[illegible] are also given [illegible].

In addition, a plot of [illegible] the same sets of data is presented in Figure [illegible].

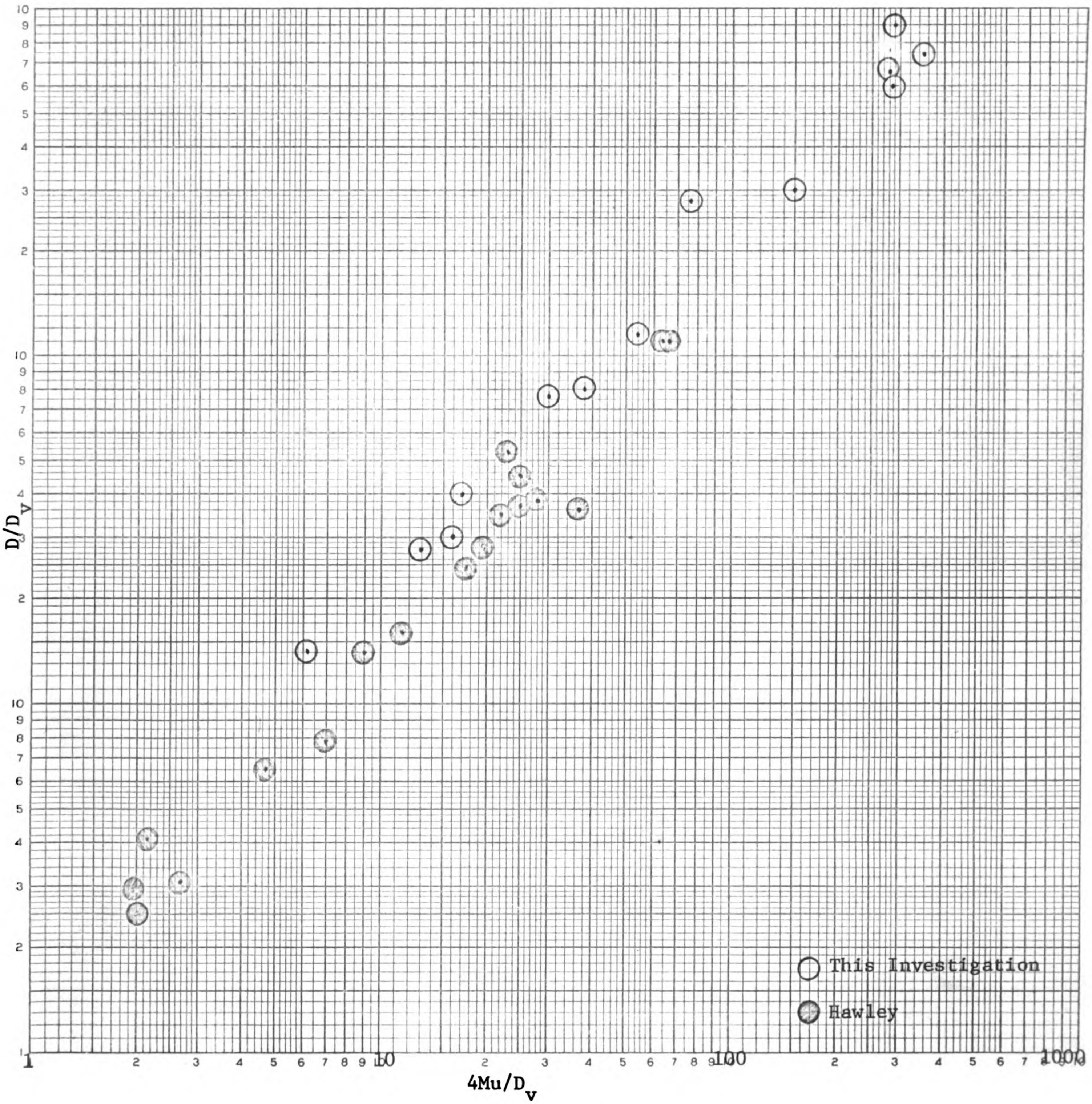

Figure XII. $4Mu/D_v$

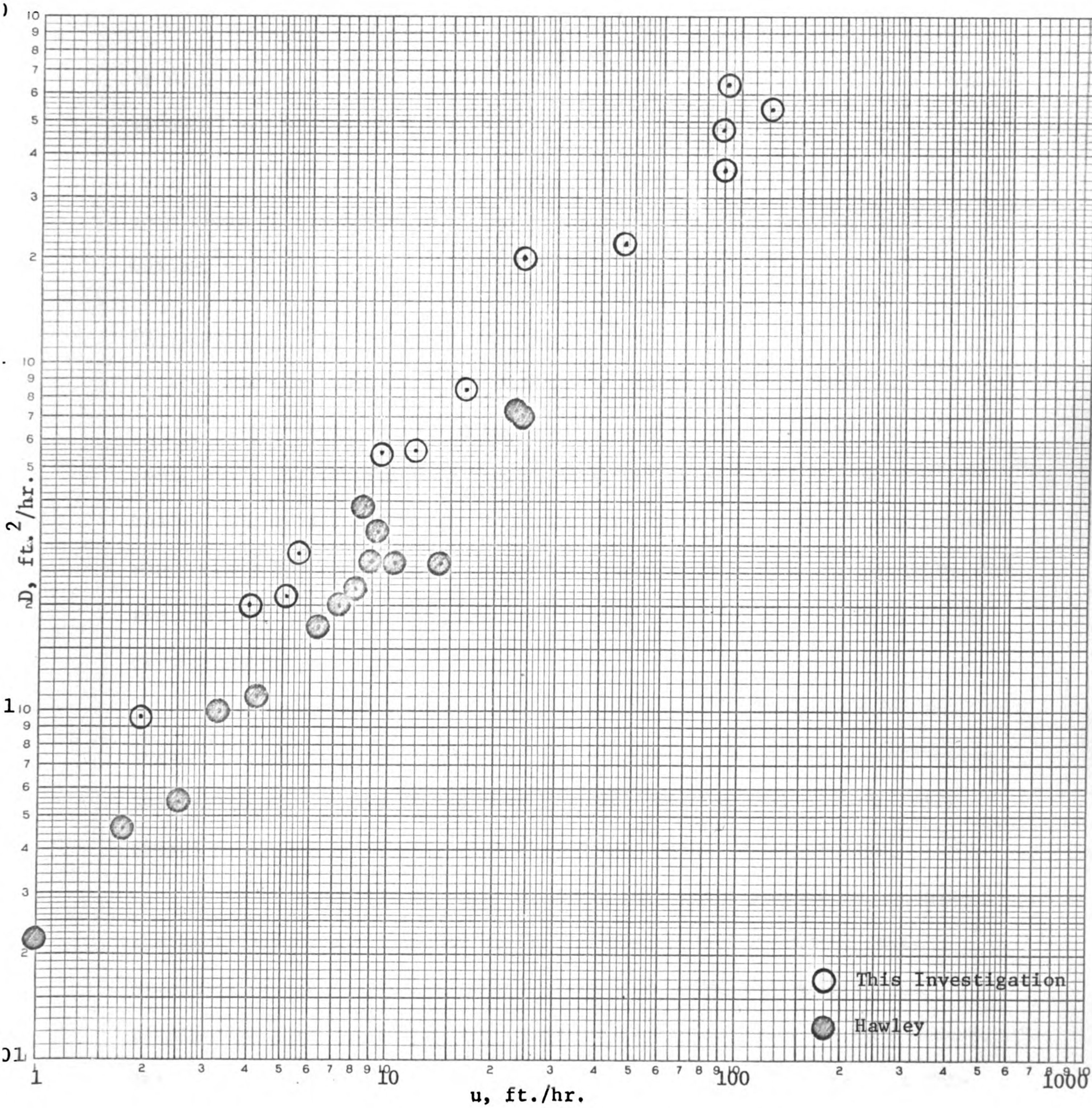

Figure XIII. Dispersion vs Fluid Velocity

Calculation of the Effective Particle Diameter

The apparatus used for this determination was designed and built by D. Mehta, a Graduate Assistant at Michigan State University. The results obtained are presented in Table I.

As shown, the value of d_{effec} was found to be 0.00497 in. This was very close to the diameter of the spherical beads (0.00414 in.) used by Hawley.[6]

Discussion of the Dispersion Coefficient Data

The data collected for this study can be found in Table II.

Figure XIII shows a significant increase in the dispersion coefficient for the irregularly shaped particles compared to the spherical beads. The actual difference in the diffusivities is somewhat greater than shown since the non-spherical particles have slightly smaller diameters than the spheres. That is, the diffusivity usually decreases with diminishing particle size.

This increase in the diffusion coefficient is substantiated in Figure XII. This graph takes particle diameter, and packing void fraction into consideration and it has been reported that the data for similarly shaped particles of varying size should fall on one straight line.[6]

It is important to note, however, that these results do not conclusively answer the question regarding stagnant and turbulent fluid presented in the theoretical discussion. One reason for this is the possibility that the proper data correlation methods have not been considered. For example, the concept of the effective particle diameter used in this work, has not been derived from a theoretical consideration of the problem under investigation. It is therefore conceivable that some other, more

appropriate, measure of particle size should be employed.

Run	Pressure Drop, ΔP in. Hg.	Flow Rate, V_o ml./min.	$V_e/\Delta P$ ml./min. in. Hg.
1	19.1	37.8	1.98
2	18.9	37.2	1.97
3	17.3	35.0	2.02
4	17.3	34.7	2.00
5	12.0	23.0	1.92
6	12.0	24.5	2.04
7	12.0	24.0	2.00
8	11.3	22.3	1.98
9	7.0	13.5	1.93
10	6.9	14.4	2.09
11	5.2	10.1	1.94

$$(V_e/\Delta P)_{ave} = 1.99 \text{ ml./min. in. Hg.}$$

TABLE I. Effective Particle Diameter Data

Run	D - ft.^{2}/hr.	u - ft./hr.	D/D_v	$4Mu/D_v$
1	0.533	112.0	7480	355
2	0.634	91.4	8900	289
3	0.356	89.6	4990	284
4	0.475	87.8	6660	278
5	0.218	46.5	3060	147
6	0.204	23.8	2860	75.4
7	0.0835	16.5	1170	52.3
8	0.0562	11.8	788	37.4
9	0.0554	9.43	777	29.9
10	0.0280	5.54	393	17.5
11	0.0211	5.08	296	16.1
12	0.0198	4.00	278	12.7
13	0.0099	1.95	139	6.18

TABLE II. Dispersion Coefficient Data

CONCLUSIONS

For flow rates between one and one-hundred feet per hour, the axial dispersion in a packed bed is affected by the shape of the packing particles. More specifically, for particles with diameters of order of magnitude 10^{-3} in., the diffusivity increases as the shape of the packing material becomes more random.

APPENDIX

[illegible]

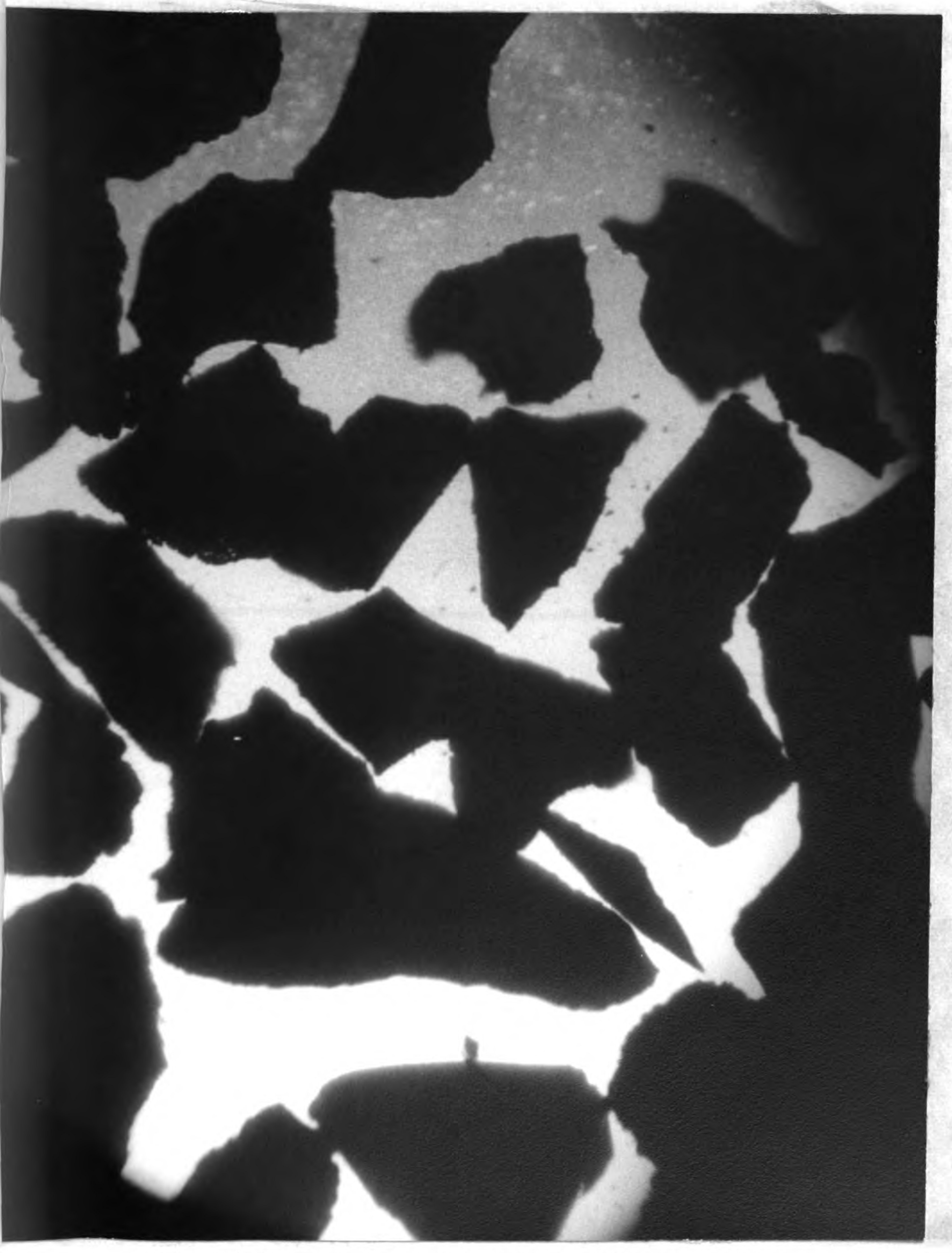

FIGURE I-I. Microphotograph of Activated Carbon Particles

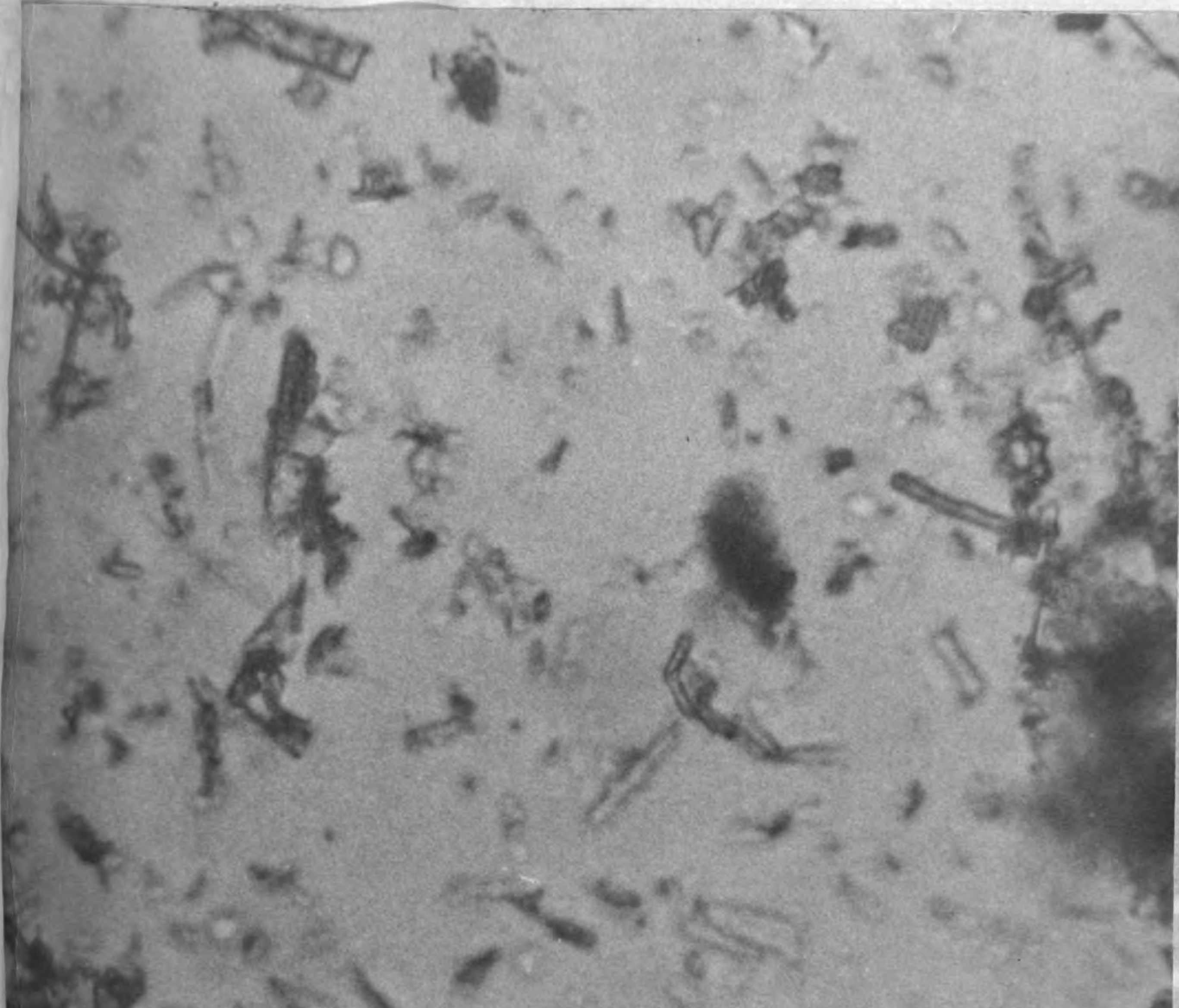

FIGURE I-II. Microphotograph of Diatomaceous Earth Particles

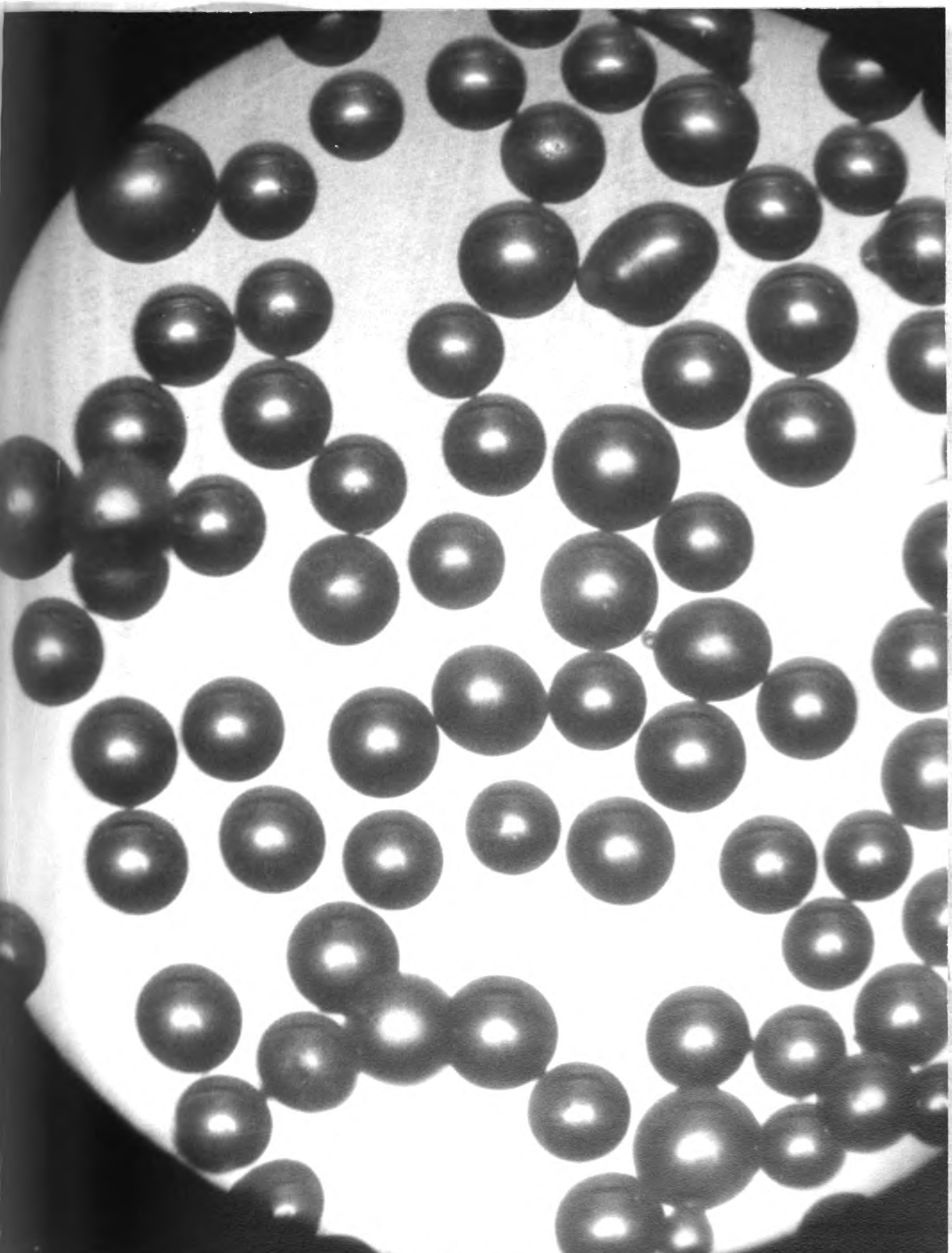

FIGURE I-III. Microphotograph of Spherical Particles

FIGURE I-IV. Microphotograph of Irregular Particles

BIBLIOGRAPHY

1. Aris, R., and Amundson, N. R., A.I.Ch.E. Journal, 3, 280, 1957.

2. Bird, R. B., et.al., Transport Phenomena, John Wiley and Sons, Inc., New York, 199, 1960.

3. Carberry, J. J., A.I.Ch.E. Journal, 4, 13M, 1958.

4. Carberry, J. J., and Bretton, R. H., A.I.Ch.E. Journal, 4, 367, 1958.

5. Eskinazi, S., Principles of Fluid Mechanics, Allyn and Bacon, Inc., Boston, 291, 1962.

6. Hawley, M. C., Solute Dispersion in Liquid-Solid Chromatographic Columns, Doctoral Dissertation, Michigan State University, 1964.

7. International Critical Tables, McGraw-Hill Book Co., Inc., New York.

8. Jacques, G., and Vermeulen, T., Longitudinal Dispersion in Solvent Extraction Columns: Peclet Numbers for Ordered and Random Packings, University of California, Berkeley, USAEC, 1957.

9. Kramers, H., and Alberda, G., Chem. Eng. Sci., 2, 173, 1953.

10. McHenry, K. W., and Wilhelm, R. H., A.I.Ch.E. Journal, 3, 83, 1957.

11. Prausnitz, J. M., A.I.Ch.E. Journal, 4, 14M, 1958.

12. Roemer, R., et. al., I. and E.C. Fund., 1, 287, 1952.

13. Taylor, G. I., Proc. Roy. Soc., A223, 446, 1954.

14. Taylor, G. I., Proc. Roy. Soc., A219, 186, 1953.